Journal of Engineering Science and Technology
Vol. 17, No. 4 (2022) 2496 - 2511

ADSORPTION OF COPPER IONS ONTO RICE HUSK ACTIVATED CARBON PREPARED USING ULTRASOUND ASSISTANCE: OPTIMIZATION BASED ON STEP-BY-STEP SINGLE VARIABLE KNOCKOUT TECHNIQUE

A. MUSLIM[1,*], E. PURNAWAN[1], NASRULLAH[1], H. MEILINA[1], MUHAMMAD Y. AZWAR[1], NUR O. DERI[2], A. KADRI[3]

[1]Department of Chemical Engineering, Faculty of Engineering, Universitas Syiah Kuala, Banda Aceh, 23114, Indonesia
[2]Department of Material Engineering, Faculty of Engineering, Universitas Malikussaleh, Muara Batu, Aceh Utara, 24351, Indonesia
[3]School of Chemical Engineering, College of Engineering, Universiti Teknologi MARA (UiTM) 40450 Shah Alam Malaysia
*Corresponding Author: abrar.muslim@che.unsyiah.ac.id

Abstract

This study proposed 3 types of rice husk activated carbon prepared by a variation of chemical activation techniques includes non-stirred, mechanical stirred and mechanical stirred with ultrasound assistance. FTIR transmission spectra showed that aromatic rings and alkenes were released more on husk activated carbon with ultrasound assistance in chemical activation (RH-ACMUS), and SEM images confirmed that more pores were obtained in RH-ACMUS. The effect of independent variables on adsorption capacity of Cu(II) ions was investigated. An optimum condition of batch mode adsorption was obtained based on step-by-step single variable knockout technique, which consisted of 500.09 mg/L of Cu(II) ions in 100 mL of aqueous volume, 1 g of RH-ACMUS, at 100-rpm magnetic stirring, pH 6, 1 atm and 27 °C. The adsorption capacity in the optimum condition was 39.84 mg/g. Adsorption of Cu(II) ions onto RH-ACMUS fitted very well (R^2 = 0.99) with pseudo-second order kinetic, and the adsorption rate and equilibrium capacity determined were 0.88 g/mg.min and 39.84 mg/g, respectively. In addition, it was best fit (R^2 = 0.91) to Freundlich adsorption isotherm with porous volume obtained was 1.52 L/mg, and adsorption intensity was 1.46, and it indicated physical adsorption was taking place dominantly.

Keywords: Rice husk, Activated carbon, Copper, Ultrasound, Kinetics, Isotherm.

1. Introduction

Pollution of heavy metal ions in liquid phase can damage the environment [1, 2], and it can cause negative impacts to human and animal because of its non-biodegradability and toxicity [3]. It caused dysfunctions of tissues and organs in human body [4, 5]. Waste-water consisting heavy metal ions mostly might be released from industrial practices, agricultural processing, domestic waste [1, 6] and educational and research centers [7].

Among separation process, adsorption would be the better method due to its effectiveness and simplicity for heavy metal ions removal including Cu(II) ions in municipal wastewater and industrial effluents [8, 9]. Some lignocellulosic waste-based adsorbents were proposed for Cu(II) ion adsorption, which had been prepared from areca catechu shell [10], barley straw [11], Chara Sp. Algae [12], wheat straw [13], sunflower leaves [14] and palm oil fruit shells [15]. Activated carbon based on lignocellulosic waste have been developed to answer the need of activated carbon was expected to reach more than 5,500 kilo ton by 2022 in global market [16]. Thus, it offers great prospect to develop low cost and better activated carbon. An excessive arrangement of studies on lignocellulosic solid waste to produce it have been investigated for adsorption and removal of Cu(II), such as areca catechu stem [17], myristica fragrans shell [18], pithecellobium jiringa shell [19], Australian pine cones [20], corncob [21], stones of Tunisian date [22], cassava peel [23], hazelnut and pecan shell [24, 25], hazelnut husks [26], coconut shell [27-29] and apricot stone [30].

Global production of RH was expected to continuously increase since the annual total world production and consumption of paddy rice have been risen with the 2 biggest contributors namely China (over 210 million metric tons) and India (over 177 million metric tons) in 2019 [31]. Rice husk which consists generally of lignin (20%), hemicellulose (20%) and cellulose (32%), organic component such as fat and crude protein (20%) [32], is a promising lignocellulosic solid waste for an adsorbent. Modified rice husk (RH) without carbonation have been proposed for removal of copper and lead ions (tartaric acid-modified RH) [33], manganese, lead and arsenic ions (iron and aluminum-impregnated RH ash) [34], divalent metal ions of copper, lead, cadmium and zinc ions (nitric acid and potassium carbonate RH [35] and copper ions (sodium hydroxide-modified RH) [36]. Meanwhile, modified RH with heat treatment have been applied for adsorption of chromium ions (ozone activation in carbonized-RH) [37], copper ions (RH heated 300-500 °C) [38], iron, manganese, zinc, copper, cadmium, and lead ions (350 °C carbonation physically and KOH-chemically activated RH) [39], hexavalent chromium ions by non-hydrothermal carbonized RH [40] and hydrothermal carbonized RH [41], lead ions (600-800 °C carbonation physically and sodium hydroxide-chemically activated RH) [42], and lead and copper ions (500 °C calcined physically RH) [43].

Previous studies had been carried on with various techniques of treatment, synthesis and preparation including physical, chemical, and physicochemical methods are applied for the production of rice husk activated carbon (RH-AC) [44-47]. The preparation of RH-AC by physicochemical activation has also been effectively applied to increase surface area and adsorption capacity [48]. Using NaOH and KOH in physicochemical activation of RH-AC produced high surface

area of 2681 m^2/g for supercapacitor application [49]. However, ultrasound assistance has not been applied in chemical activation of RH-AC.

Meanwhile, ultrasound assistance in a batch mode adsorption increased 4-dodecylbenzene sulfonate adsorption onto corn cob-AC [21], and it increased adsorption of copper by melon waste-AC [50]. Interestingly, ultrasound assistance (1 MHz of ultrasonic probe) in an AC chemical activation increased adsorption of copper by pithecellobium jiringa-AC [19]. Response surface methodology (RSM) was mostly applied to achieve an optimum condition of independent variables in adsorption, and it recommended a minimal number of experiments to run [17, 51]. Step-by-step single variable knockout technique, which is used in present study, has not been proposed in previous studies. This technique can be minimized the number of experiments to run. To be fairly compared with the RSM number of experiments without repetition, each experiment was run without repetition.

This study proposed a preparation of RH-AC by physicochemical activation whereas the physical activation was conducted in a tube furnace, and the chemical activation were carried out using NaOH with 40 kHz ultrasound assistance in ultrasonic bath. Functional groups and morphology of rice husk-based activated carbons were analysed by FTIR and SEM techniques, respectively. The adsorption capacity over independent variables such as adsorption time, initial pH, initial Cu(II) ions concentration and adsorption temperature were investigated, and an optimum condition to attain a maximum adsorption was obtained based on step-by-step single variable knockout technique. All the parameters of adsorption kinetics and adsorption isotherms were determined at the optimum condition.

2. Materials and Method

2.1. Preparation and characterization of activated carbon

RH of 1 kg was collected from a paddy milling. To remove RH impurities washed and decanted using tap water. Then, RH then was washed with RO water to finally clean it from the impurities. After washing the cleaned RH were dried at 120 °C for 3 h in an oven (Memmert NN-ST342M, Western Germany). The dried RH of 250 g was then pyrolysed at 500 °C with heating and N_2 injection rate of 45 °C/min and 5 ml/min respectively for 30 min physical activation using a furnace (TF-120, 300-1500 °C, Human Lab Inc., Korea) [17]. After physical activation, RH carbon was ball milled into powder and sieved (ASTM standard) to 60-80 mesh size [33].

RH carbon (activated physically) of 50 g was activated chemically using 500 mL NaOH (97%, from Aldrich) at 0.5 M in a beaker glass (750-mL) without mechanical stirring, or not stirred (NS) for 1 hour at room temperature 27 °C (± 1 °C). RH-AC was washed using RO water and filtered, it was repeated many times until the pH of remaining water reaching neutral (pH 7 ± 0.1). RH-AC was vacuum-filtered and dried at 110 °C until for 5 hours. Finally, RH-AC was stored in a sealed bottle and labelled as RH-ACNS.

The chemical activation procedure was repeated for other 50 g of RH carbon with mechanical stirring (MS) at 75-rpm (IKA, type C-MAG HS 7) for the same activating time of 1 hour. This RH-AC was labelled as RH-ACMS. The chemical activation procedure was repeated for other 50 g of RH carbon with mechanical

stirring at 75-rpm under 40 kHz ultrasound assistance (ultrasonic bath, Bransonic 8510, 40 kHz, USA) for the same activating time of 1 hour at room temperature 27 °C (± 1 °C). This RH-AC was labelled as RH-ACMUS.

2.2. Characterization of RH-ACNS, RH-ACMS and RH-ACMUS

Fourier Transform Infrared Spectroscopy (FTIR, Shimadzu Prestige 21, Japan) technique was applied to identify the chemical functional groups of RH-ACNS, RH-ACMS and RH-ACMUS. The FTIR spectrums were quantified at the range of 400-4000 cm^{-1} using KBr Pellet method. Each sample of 0.5 mg was well mixed by finely pulverizing it with 500 mg of KBr. The mixture was slow dried at 110 °C (± 1 °C), and it was put into a 13 mm-diameter pellet-forming die to form transparent pellets in vacuum condition. Then, the pellet was used to measure the infrared spectra of RH-ACNS, RH-ACMS and RH-ACMUS. Scanning Electron Microscopy (SEM, HITACHI TM3000, Japan) was used to capture the surface morphology of RH-ACNS, RH-ACMS and RH-ACMUS at 50/60Hz and 1 phase of 500VA accelerating voltage. Before conducting SEM analysis, each sample was dried at 105 °C for 20 min in the Memmert oven.

2.3. Adsorption experiments

Batch experiments were conducted using a beaker glass (150 mL to contact the activated carbon with an artificial solution of $CuSO_4.5H_2O$ (99% pure from Aldrich). The stock solution (1000 mg/L) prepared and analysed using Atomic Absorption Spectrophotometer (AAS, Shimadzu AA 6300, Japan) [18, 20]. Adsorption time was varied for 0, 15, 30, 45, 60, 75 and 90 min with 100-rpm magnetic stirring speed. The activated carbon-solution systems were set at 49.92-500.15 mg/L of initial Cu(II) concentration, 4-6 of initial pH, 1 g of activated carbon and 27-47 °C of adsorption temperature. The result of each experiment was analysed in triplicate run of AAS with the value of standard deviation (STDEV) being less than 2%. Effect of all the independent variables were investigated, and an optimum condition was obtained based on step-by-step single variable knockout (S^3V-KO) technique wherein a maximum adsorption capacity was worked out. The S^3V-KO technique was presented in Table 1 of Results and Discussion part. The optimum condition was used for adsorption kinetics and adsorption isotherms.

Adsorption capacity at a certain time was obtained using Eq. (1) which was modified from previous study [52, 53]:

$$q_{t=n} = \frac{(C_{t=0} - C_{t=n})}{m_{AC}} V_S \quad (1)$$

where $C_{t=0}$ (mg/L) is Cu(II) concentration at the time of zero (t=0 min), $C_{t=0} = C_0$ (initial Cu(II) concentration; $C_{t=n}$ (mg/L) is Cu(II) concentration at any time of n (min); $q_{t=n}$ (mg/g) is adsorption capacity at $t=n$; V_S (L) denotes as the batch mode volume (L); and m_{AC} (g) is the activated carbon mass.

All the parameters of adsorption kinetics and adsorption isotherms were determined at an optimum condition. The linearized pseudo-first order kinetic (LPFOK) model of Lagergren model [54] and the linearized pseudo-second order kinetic (LPSOK) model of Ho model were presented by Eq. (2) and (3), respectively [20, 55, 56]:

$$\log(q_e - q_t) = \log q_e - \left(\frac{k_L t}{2.303}\right) \quad (2)$$

$$\frac{t}{q_t} = \frac{1}{k_H {q_e}^2} + \frac{t}{q_e} \quad (3)$$

where q_t (mg/g) is $q_{t=n}$; k_L (/min) and k_H (g/mg.min) are the rate constant of LPFOK and LPSOK, respectively; and q_e (mg/g) represents adsorption capacity at equilibrium time (t_e). The linearized Langmuir model [57] (LLM) of Eq. (4) and the linearized Freundlich model [58] (LFM) of Eq. (5) were taken into account to study adsorption isotherm [20, 56]:

$$\frac{C_e}{q_e} = \frac{1}{q_m K_L} + \frac{1}{q_m} C_e \quad (4)$$

$$\log q_e = \frac{1}{n} \log C_e + \log K_F \quad (5)$$

where C_e (mg/L) symbolizes equilibrium Cu(II) concentration; q_m (mg/g) represents the maximum adsorption capacity of LLM monolayer; K_L (L/mg) is LFM-based porous volume constant; K_F (L/mg) indicates LFM-based porous volume constant; and n is LFM-based adsorption intensity.

3. Results and Discussion

3.1. FTIR spectra of activated carbon

The FTIR spectra of RH-ACNS, RH-ACMS and RH-ACMUS at 400 to 4000 cm^{-1} are shown in Fig. 1 where it highlights 4 functional groups. The characteristic bands are the =C–H bending at 680-860 cm^{-1} (aromatic) with a peak at 806 cm^{-1}; C–O bending at 1012-1309 cm^{-1} (carboxylic acids, ethers and ester) with a peak at 1007 cm^{-1}; C=C bending at 1500-1700 cm^{-1} (aromatic rings) with a peak at 1554, 1697 cm^{-1}; and C–H bending at 3010-3100 cm^{-1} (alkenes) [53] with a peak at 3024 cm^{-1} [35, 37, 38, 56].

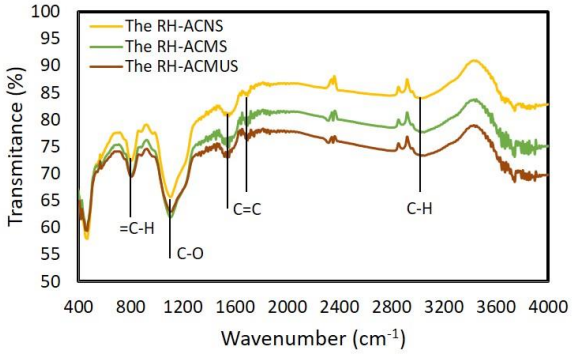

Fig. 1. FTIR spectra of activated carbon.

Overall, FTIR results confirmed that mechanical stirring in the chemical activation of activated carbon reduces the transmittance of functional groups of aromatic rings from 80.61 (RH-ACNS) to 74.55 % (RH-ACMS), and alkenes from 84.05 (RH-ACNS) to 77.71 % (RH-ACMS). The effect of ultrasound was clearly shown by RH-ACMUS transmission spectra where it reduces the transmittance of aromatic rings and alkenes to 72.94 and 73.31 %, respectively. This reduction

corresponds to the destruction of the hydrogen bonds of the aromatic and alkene as it exposes to the ultrasound wave [59, 60].This subsequently releases more volatile matters in RH-ACMUS thus leading to more potential pores [19].

3.2. SEM micrographs of activated carbon

As shown in Fig. 2, surface morphology of activated carbon varies between preparation techniques where more pores were observed by the assistance of the ultrasound wave as shown in RH-ACMUS compared to RH-ACNS and RH-ACMS. This is possibly due to the effect of the ultrasound wave which accelerates the NaOH dehydrating agent to break the stretch and bending of chemical functional group leading to more volatile matters being released from the activated carbon. This result was in line with the FTIR observation presented in section 3.1 as well as from the previous studies [19, 59, 60]. Thus, more Cu(II) is most likely to be absorbed by RH-ACMUS rather than in RH-ACNS and RH-ACMS.

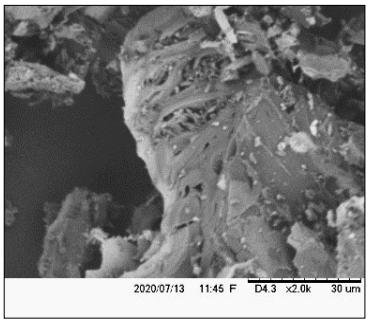

(a) RH-ACNS

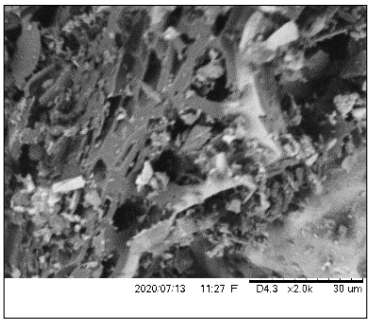

(b) RH-ACMS

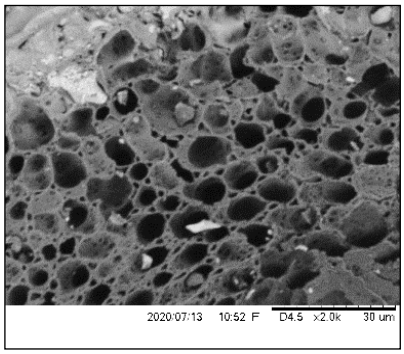

(c) RH-ACMUS

Fig. 2. SEM micrographs of activated carbon.

3.3. Effect of contact time on q_t

The first stage of obtaining an optimum condition of adsorption was to work out the value of t_e for the 3 types of the rice husk activated carbon prepared. The effect of contact time on q_t was evaluated in this stage, and the results were shown in Fig. 3 where RH-ACNS and RH-ACMS curves present the same trend of adsorption capacity where it increases slowly in the first 60-min contact time. Then it increases

moderately from 24.97 to 25.09 mg/g at 60-min and 75-min, respectively for RH-ACNS and from 29.09 to 30.51 mg/g at 60-min and 75-min, respectively for RH-ACMS. Subsequently, the increment subdued at 90-min to reach equilibrium adsorption capacity of 25.07 and 30.61 mg/g for RH-ACNS and RH-ACMS, respectively. Interestingly, the rate of adsorption capacity of RH-ACMUS escalated sharply in the first 15-min contact time with an amount of39.71 mg/g. Following to that the adsorption of Cu(II) starts to stabilize with 39.78 and 39.82 mg/g at 30 and 45 min, respectively and finally reached to 39.84 mg/g at 90-min. Similar trend of the Cu(II) adsorption capacity were also reported in the previous studies [19, 33]. From this stage, 90-min contact time was selected as t_e, and only RH-ACMUS was used for the rest batch experiments as it showed the highest q_e.

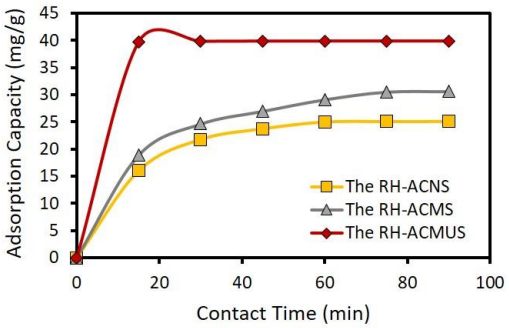

Fig. 3. Effect of contact time on q_t. Batch condition: V_S = 100 mL, C_0 = 500.15 mg/L, m_{AC} = 1 g, 100-rpm, pH 6, 1 atm, 27 °C.

3.4. Effect of C_0 on q_e

As revealed in Fig. 4, the value of q_e for RH-ACMUS increases as C_0 increases from 49.92 to 250.12 mg/L. The value of q_e jumped by 112.99 % for C_0 increment from 250.12 to 500.09 mg/L. Similar inclination trend was also reported in the earlier work [19, 21]. This trend is reasonable because q_e should increase continuously with C_0 increment, and it increases insignificantly just before all active sites being occupied by the adsorbate [53, 54].

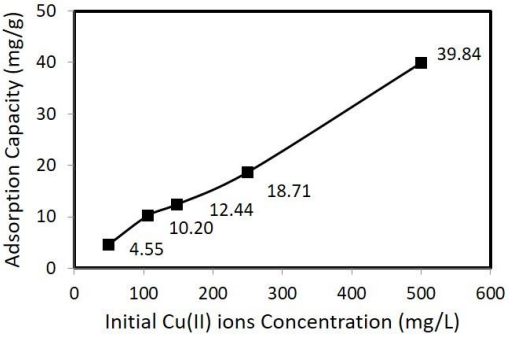

Fig. 4. Effect of C_0 on q_e. Batch condition: V_S = 100 mL, C_0 = 49.92-500.15 mg/L, m_{AC} = 1, 100-rpm , pH 6, 1 atm, 27 °C.

3.5. Effect of initial pH on q_e

To investigate the effect of initial pH on q_e, the initial pH of Cu(II) solution was adjusted by dropping 0.01 M NaOH, or 0.01 M HCl [18] before RH-ACMUS was added into the Cu(II) solution. The highest q_e in Cu(II) adsorption was generally obtained in acid condition, and it could be linear and parabolic trend over initial pH under 7 [18, 22, 24, 50]. As highlighted in Fig. 5, rising initial pH from 4 to 5 resulted in the increment of q_e by 44.25 %, and it was by 191.78 % for the increase of initial pH from 5 to 6. Therefore, maximum q_e of Cu(II) on RH-ACMUS was taking place at pH 6.

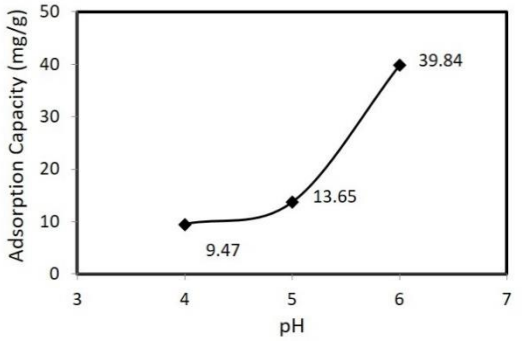

Fig. 5. Effect of initial pH on q_t. Batch condition: V_S = 100 mL, C_0 = 500.15 mg/L, m_{AC} = 1, 100-rpm, pH 4-6, 1 atm, 27 °C.

3.6. Effect of temperature on q_e

Figure 6 shows the effect of temperature on q_e where it displays a sharp decline by 66.17 % when the temperature changes from 27 to 37 °C, and subsequently, the value of q_e decreases to 11.41 mg/g at 47 °C. Such trend is in accordance with the previous experimental results reported earlier [18, 19] at which proves that physical adsorption of Cu(II) occurred in RH-ACMUS. This was also supported by the previous discussion (t versus q_t) in section 3.3 whereas Cu(II) adsorption on RH-ACMUS occurred faster indicating physical adsorption [61].

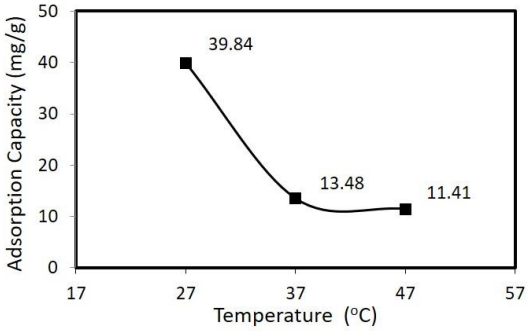

Fig. 6. Effect of temperature on q_t. Batch condition: V_S = 100 mL, C_0 = 500.15 mg/L, m_{AC} = 1, 100-rpm, pH 4-6, 1 atm.

Table 1. The S^{3}V-KO technique for batch experiments.

Dependent and Independent Variables of Batch Experiments							
	C_0 = 500.15 mg/L, m_{AC} = 1 g, 100-rpm, pH 6, 1 atm, 27 °C						
		t (min)					
		15	30	45	60	75	90
q_e (mg/g)	RH-ACNS	16.02	21.77	23.73	24.97	25.05	25.07
	RH-ACMS	18.88	24.61	26.95	29.09	30.51	30.61
	RH-ACMUS	39.71	39.78	39.82	39.83	39.83	**39.84**
Reduction		**t = 15-75 min, RH-ACNS and RH-ACMS**					
Selected		t_e = 90 min, RH-ACMUS					
	m_{AC} = 1 g, 100-rpm, pH 6, 1 atm, 27 °C						
		C_0 (mg/L)					
			49.92	106.66	148.26	250.12	500.09
q_e (mg/g)	RH-ACMUS	t_e 90 min	4.55	10.20	12.44	18.71	**39.84**
Reduction		C_0 49.92-250.12 mg/L					
Selected		C_0 500.09 mg/L					
	m_{AC} = 1 g, 100-rpm, 1 atm, 27 °C						
					4	**5**	**6**
q_e (mg/g)	RH-ACMUS	t_e 90 min	C_0 = 500.09 mg/L		9.47	13.65	**39.84**
Reduction		**pH 4-5**					
Selected		**pH 6**					
	m_{AC} = 1 g, 100-rpm, 1 atm						
					Temperature, T (°C)		
					47	37	27
q_e (mg/g)	RH-ACMUS	t_e 90 min	C_0 = 500.09 mg/L	pH 6	11.41	13.48	**39.84**
Reduction		T 37-47 °C					
Selected		T 27 °C					

The order of batch experiment to investigate the effect of all the independent variables on q_e being discussed above was based on the S^{3}V-KO technique presented in Table 1. Reducing step-by-step the values of single independent variable and selecting the value of single independent variable for the next step of batch experiment after the highest q_e value being obtained, were also presented in Table 1. The S^{3}V-KO technique recommended only 11 runs of experiments. Meanwhile, the RSM Box-Behnken design and RSM central composite design [17, 51] recommended 30 and 29 runs of experiments, respectively to run for each RH-AC based. It means that S^{3}V-KO technique can minimize the number of experiments compared to the RSM. Based on the S^{3}V-KO technique, an optimum condition of batch mode adsorption obtained suggests 500.09 mg/L of Cu(II) ions in 100 mL of aqueous volume, 1 g of RH-ACMUS, at 100-rpm magnetic stirring, pH 6, 1 atm pressure and temperature of 27 °C.

The optimum condition highlighted in Table 1 was used for the kinetics analysis. Figs. 7(a) and (b) display that Cu(II) adsorption capacity of RH-ACMUS fitted best to the LPSOK model (R^2 = 0.9975). Pseudo-first order kinetic model might imply chemical adsorption, or physical adsorption depending on reaction rate-

limiting mechanism, or diffusion rate-limiting behavior, respectively [62]. It referred to chemisorption for Pb(II) adsorption onto acidified carbon nanotubes [63], and methylene blue and crystal violet adsorption on Millettia thonningii seed pods-based activated carbon [64]. Meanwhile, it implied the physical adsorption for Cu(II) adsorption on activated carbon prepared from Myristica fragrans shell [18] and Pithecellobium Jiringa [19], and phenol adsorption on activated carbon utilized from Kraft lignin [65]. Based on the isotherm study it fits well with the LFM, the pseudo-first order kinetic of Cu(II) adsorption on RH-ACMUS should be controlled by diffusion rate-limiting [62]. From the intercept and slope of LPSOK model, k_H and q_e were obtained, which was 0.88 g/mg.min and 39.84 mg/g, respectively.

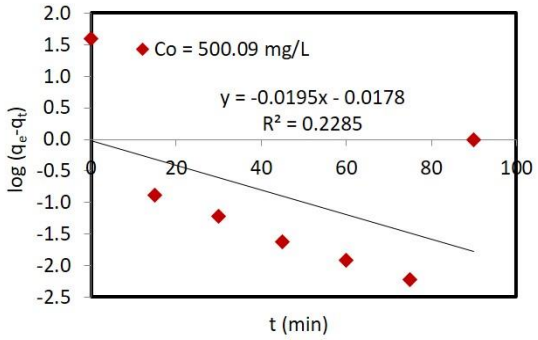

(a) Plot of LPFOK model

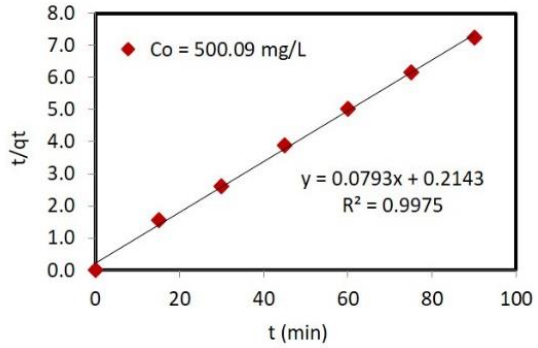

(b) Plot LPSOK model

Fig. 7. Adsorption kinetics. Batch condition: V_S = 100 mL, C_0 = 500.15 mg/L, m_{AC} = 1 g, 100-rpm, pH 6, 1 atm, and 27 °C.

3.7. Adsorption kinetics and isotherms

As clearly shown by the correlation coefficients in Fig. 8(a) and (b), the LFM adsorption isotherm fits very well to adsorption of Cu(II) on RH-ACMUS (R^2 = 0.914). As expected in the previous discussion, each active site of RH-ACMUS should adsorb more Cu(II) to form multilayer on RH-ACMUS surface. The LFM-based porous volume constant (K_F) was 1.52 L/mg, and adsorption intensity n was 1.46. Overall, it inferred that physical adsorption control dominantly the Cu(II) adsorption onto RH-ACMUS. Similar trend was also reported in the previous studies where the adsorption capacity decreases with the increase in temperature for physical adsorption [18, 19, 66].

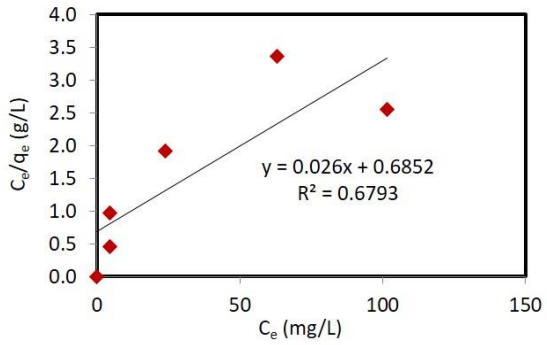

(a)

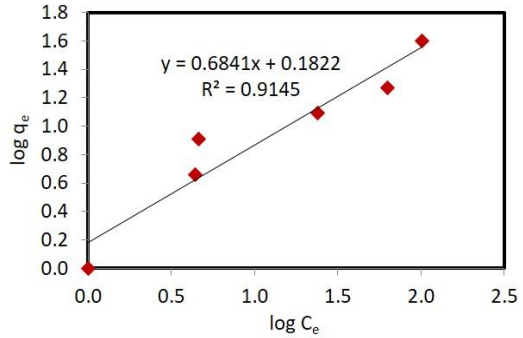

(b)

Fig. 8. (a) **Plot of LLM and (b) LFM. Experimental condition: V_S = 100 mL, C_0 = 500.09 mg/L, m_{AC} = 1 g of RH-ACMUS, 100-rpm magnetic stirring, pH 6, 1 atm, 27 °C.**

4. Conclusions

This study proposed the preparation of activated carbon from rice husk for Cu(II) adsorption. Assisting ultrasound in chemical activation resulted in more pores being obtained on the activated carbon of RH-ACMUS. The ultrasound waves caused more volatile matter being released from RH-ACMUS compared to the ones without ultrasound assistance. More pores were obtained on RH-ACMUS compared to the ones without ultrasound assistance. All the independent variables were investigated, which suggesting the optimum condition obtained using the step-by-step single variable knockout (S^3V-KO) technique which are RH-ACMUS-solution system consisted of 100 mL Cu(II) solution at 500.09 mg/L, 1 g of RH-ACMUS, 100-rpm magnetic stirring, pH 6, 1 atm and 27 °C. In the optimum condition, pseudo-second order kinetic fits very well to Cu(II) adsorption capacity of RH-ACMUS with the equilibrium adsorption capacity and rate constant of 9.84 mg/g and 0.88 g/mg.min, respectively. Freundlich adsorption isotherm provided the best fit for adsorption of Cu(II) on RH-ACMUS, and the porous volume obtained was 1.52 L/mg, and the adsorption intensity was 1.46. This clearly show that rice husk with ultrasound preparation technique in chemical activation offers a promising competitive activated carbon characteristics for the future.

References

1. Hawkes, S.J. (1997). What is a heavy metal? *Journal of Chemical Education*, 74(11), 1374-1380.
2. Bala, M.; Shehu, R.A.; and Lawal, M. (2008). Determination of the level of some heavy metals in water collected from two pollution - Prone irrigation areas around Kano Metropolis. *Bayero Journal of Pure and Applied Sciences*, 1(1), 6-38.
3. Minamisawa, M.; Minamisawa, H.; Yoshida, S.; and Takai, N. (2004). Adsorption behavior of heavy metals on biomaterials. *Journal of Agricultural and Food Chemistry*, 52(18), 5606-5615.
4. Theophanides, T.; and Anastassopoulou, J. (2002). Copper and carcinogenesis. *Critical Reviews in Oncology/Hematology*, 42(1), 57-64.
5. Kandah; Munther, I.; Fahmi, A.; Al-Rub, A.; and Al-Dabaybeh, N. (2004). The aqueous adsorption of copper and cadmium ions onto sheep manure. *Adsorption Science and Technology*, 21(6), 501-509.
6. Sardella, F.; Gimenez, M.; Navas, C.; Morandi, C.; Deiana, C.; and Sapag, K. (2015). Conversion of viticultural industry wastes into activated carbons for removal of lead and cadmium. *Journal of Environmental Chemical Engineering*, 3(1), 253-260.
7. Hassanvand, M.S.; Naddafi, K.; Nabizadeh, R.; Momeniha, F.; Mesdaghinia, A.; and Yaghmaeian, K. (2011). Hazardous waste management in educational and research centers: a case study. *Toxicological & Environmental Chemistry*, 93(8), 1636-1642.
8. Eccles, H. (1999). Treatment of metal-contaminated wastes: Why select a biological process? *Trends in Biotechnology*, 17(12), 462-465.
9. Leung, W.C.; Wong, M.F.; Chua, H.; Lo, W.; Yu, P.H.F; and Leung, C.K. (2000). Removal and recovery of heavy metals by bacteria isolated from activated sludge treating industrial effluents and municipal wastewater. *Water Science and Technology*, 41(12), 233-240.
10. Muslim, A.; Zulfian, Ismayanda, M.H.; Devrina, E.; and Fahmi H. (2015). Adsorption of Cu(II). from the aqueous solution by chemical activated adsorbent of areca catechu shell. *Journal of Engineering Science and Technology* (*JESTEC*), 10(12), 1654-1666.
11. Pehlivan, E.; Altun, T.; and Parlayici, S. (2012). Modified barley straw as a potential biosorbent for removal of copper ions. *Food Chemistry*, 135(4), 2229-2234.
12. Kalash, K.R.; Alalwan, H.A.; Al-Furaiji, M.H.; Alminshid, A.H.; and Waisi, B.I. (2020). Isothermal and kinetic studies of the adsorption removal of Pb(II), Cu(II), and Ni(II) ions from aqueous solutions using modified Chara Sp. Algae. *Korean Chemical Engineering Research*, 58(2), 301-306.
13. Dang, V.B.H.; Doan, H.D.; Dang-Vu, T.; and Lohi, A. (2009). Equilibrium and kinetics of biosorption of cadmium(II) and copper(II) ions by wheat straw. *Bioresource Technology*, 100(1), 211-219(2009).
14. Benaïssa, H.; and Elouchdi, M.A. (2007). Removal of copper ions from aqueous solutions by dried sunflower leaves. *Chemical Engineering and Processing*, 46(7), 614-622.

15. Hossain, A., Ngo, H.H.; Guo, W.S.; and Nguyen, T.V. (2012). Palm oil fruit shells as biosorbent for copper removal from water and wastewater: Experiments and sorption models. *Bioresource Technology*, 113, 97-101.
16. Activated carbon market by type (Powdered, granular, others (pelletized, bead)), Application (Liquid phase (Water treatment, foods & beverages, pharmaceutical & medical), Gaseous phase (Industrial, automotive)), Region - global forecast to 2021. Retrieved January 20, 2021, from: https://www.marketsandmarkets.com/Market-Reports/activated-carbon-362.html.
17. Muslim, A.; Marwan; Ramli, S.; Azwar, M.Y.; Darmadi; Putra, B.P.; and Rizal, S. (2019). Adsorption of Cu(II) ions on areca catechu stem-based activated carbon: Optimization using response surface methodology. *International Review on Modelling and Simulations*, 12(2), 123-129.
18. Syahiddin, D.S.; and Muslim, A. (2018). Adsorption of Cu (II) Ions onto myristica fragrans shell-based activated carbon: isotherm, kinetic and thermodynamic studies. *Journal of the Korean Chemical Society*, 62(2), 79-86.
19. Muslim, A.; Ellysa; and Syahiddin, D.S. (2017). Cu(II) Adsorption using activated carbon prepared from pithecellobium Jiringa (Jengkol) shells with ultrasonic assistance: isotherm, kinetic and thermodynamic studies. *Journal of Engineering and Technological Sciences*, 49(4), 472-490.
20. Muslim, A. (2017). Australian pine cones-based activated carbon for adsorption of copper in aqueous solution. *Journal of Engineering Science and Technology* (*JESTEC*), 12(2), 280-295.
21. Milenković, D.D.; Bojić, A.L.J.; and Veljković, V.B. (2013). Ultrasound-assisted adsorption of 4-dodecyl benzene sulfonate from aqueous solution by corn cob activated carbon. *Ultrasonics Sonochemistry*, 20(3), 955-962.
22. Bouhamed, F.; Elouear, Z.; and Bouzid, J. (2012). Adsorptive removal of copper (II) from aqueous solutions on activated carbon prepared from Tunisian date stones: equilibrium kinetics and thermodynamics. *Journal of the Taiwan Institute of Chemical Engineers*, 43(5), 741-749.
23. Moreno-Pirajan, J.C.; and Giraldo, L. (2010). Adsorption of copper from aqueous solution by activated carbons obtained by pyrolysis of cassava peel. *Journal of Analytical and Applied Pyrolysis*, 87(2), 188-193.
24. Demirbas, E.; Dizge, N.; Sulak, M.T.; and Kobya, M. (2009). Adsorption kinetic and equilibrium of copper from aqueous solution using hazelnut shell activated carbon. *Chemical Engineering Journal*, 148(2-3), 480-487.
25. Klasson, K.T.; Wartelle, L.H.; James, E.; Rodgers, J.E; and Lima, I.M. (2009). Copper(II) adsorption by activated carbons from pecan shells: Effect of oxygen level during activation. *Industrial Crops and Products*, 30(1), 72-77.
26. Imamoglu, M.; and Tekir, O. (2008). Removal of copper (II) and lead (II) ion from aqueous solution by adsorption on activated carbon from a new precursor hazelnut husks. *Desalination*, 228(1–3), 108-113.
27. Fang, X.; Xu, X.; Wang, S.; and Wang, D. (2013). Adsorption Kinetics and Equilibrium of Cu(II) from Aqueous Solution by Polyaniline/Coconut Shell–Activated Carbon Composites. *Journal of Environmental Engineering*, 139(10), 1279-1284.
28. Moreno-Piraján, J.C.; Garcia-Cuello, V.S.; and Giraldo, L. (2011). The removal and kinetic study of Mn, Fe, Ni and Cu ions from wastewater onto activated

carbon from coconut shells. *Adsorption*, 17, 505-514.

29. Qin, Q.; Wu, X.; Chen, L.; Jiang, Z.; and Xu, Y. (2018). Simultaneous removal of tetracycline and Cu(II) by adsorption and coadsorption using oxidized activated carbon. *RSC Advances*, 8, 1744-1752.
30. Kobya M.; Demirbas E.; Senturk E.; and Ince, M. (2005). Adsorption of heavy metal ions from aqueous solutions by activated carbon prepared from apricot stone. *Bioresource Technology*, 96(13), 1518-1521.
31. Paddy rice production worldwide 2019, by country. Retrieved January 27, 2021, from https://www.statista.com/statistics/255937/leading-rice-producers-worldwide/.
32. Songlei, L.V.; Chunxi, L.I.; Jianguo, M.I.; and Hong, M. (2020). A functional activated carbon for efficient adsorption of phenol derived from pyrolysis of rice husk, KOH-activation and EDTA-4Na-modification. *Applied Surface Science*, 510, 145425.
33. Wong, K.K.; Lee, C.K.; Low, K.S.; and Haron, M.J. (2003). Removal of Cu and Pb by Tartaric Acid Modified Rice Husk from Aqueous Solution. *Chemosphere*, 50(1), 23-28.
34. Abo-El-Enein, S.A.; Eissa, M.A.; Diafullah, A.A.; Rizk, M.A.; and Mohamed, F.M. (2009). Removal of some heavy metals ions from wastewater by copolymer of iron and aluminum impregnated with active silica derived from rice husk ash. *Journal of Hazardous Materials*, 172(2–3), 574-579.
35. Akhtar, M.; Iqbal, S.; Kausar, A.; Bhanger, M.I.; and Shaheen, M.A. (2010). An economically viable method for the removal of selected divalent metal ions from aqueous solutions using activated rice husk. *Colloids and Surfaces B: Biointerfaces*, 75(1), 149-155.
36. Priyantha, N.; Sandamali, H.K.W.; and Kulasooriya, T.P.K. (2018). Sodium hydroxide modified rice husk for enhanced removal of copper ions. *Water Science and Technology*, 78(7), 1615-1623.
37. Sugashini, S.; and Begum, K.M.M.S. (2015). Preparation of activated carbon from carbonized rice husk by ozone activation for Cr(VI) removal. *New Carbon Materials*, 30(3), 252-261.
38. Nakbanpote, W.; Goodman, B.A.; and Thiravetyan, P. (2007). Copper adsorption on rice husk derived materials studied by EPR and FTIR. *Colloids and Surfaces A: Physicochemical and Engineering Aspects*, 304(1–3), 7-13.
39. Daifullah, A.A.M.: Girgis, B.S.; and Gad, H.M.H. (2003). Utilization of agro-residues (rice husk) in small waste water treatment plans. *Materials Letters*, 57(11), 1723-1731.
40. Mullick, A.; Moulik, S.; and Bhattacharjee, S. (2018). Removal of Hexavalent Chromium from Aqueous Solutions by Low-Cost Rice Husk-Based Activated Carbon: Kinetic and Thermodynamic Studies. *Indian Chemical Engineer*, 60(1), 58-71.
41. Ding, D.; Ma, X.; Shi, W.; Lei, Z.; and Zhang, Z. (2016). Insights into mechanisms of hexavalent chromium removal from aqueous solution by using rice husk pretreated using hydrothermal carbonization technology. *RSC Advances*, 6, 74675-74682.
42. Hassan, A.F.; and Youssef, A.M. (2014). Preparation and characterization of microporous NaOH-activated carbons from hydrofluoric acid leached rice husk and its application for lead(II) adsorption. *Carbon Letters*, 15(1), 57-66.

43. Vieira, M.G.A.; de Almeida Neto, A.F.; da Silva, M.G.C.; Carneiro, C.N.; and Melo Filho, A.A. (2014). Adsorption of lead and copper ions from aqueous effluents on rice husk ash in a dynamic system. *Brazilian Journal of Chemical Engineering*, 31(2), 519-529.
44. Kumagai, S.; Shimizu, Y.; Toida, Y.; and Enda, Y. (2009). Removal of dibenzothiophenes in kerosene by adsorption on rice husk activated carbon. *Fuel*, 88(10), 1975-1982.
45. Malik, P. (2003). Use of activated carbons prepared from sawdust and rice-husk for adsorption of acid dyes: a case study of Acid Yellow 36. *Dyes and Pigments*, 56(3), 239-249.
46. Asadullah, M.; Kabir, M.S.; Ahmed, M.B.; Razak, N.A.; Rasid, N.S.A.; and Aezzira, A. (2013). Role of microporosity and surface functionality of activated carbon in methylene blue dye removal from water. *Korean Journal of Chemical Engineer*, 30(12), 2228-2234.
47. Alvarez, J.; Lopez, G.; Amutio, M.; Bilbao, J.; and Olazar, M. (2015). Physical activation of rice husk pyrolysis char for the production of high surface area activated carbons. *Industrial & Engineering Chemistry Research*., 54(29), 7241-7250.
48. Prapagdee, S.; Piyatiratitivorakul, S.; and Petsom, A. (2016). Physico-chemical Activation on Rice Husk Biochar for Enhancing of Cadmium Removal from Aqueous Solution. *Journal of Water, Environment and Pollution*, 13(1), 27-34.
49. Muniandy, L.; Adam, F.; Mohamed, A.R.; and Ng, E.P. (2014). The synthesis and characterization of high purity mixed microporous/mesoporous activated carbon from rice husk using chemical activation with NaOH and KOH. *Microporous Mesoporous Materials*, 197, 316-323.
50. Gupta, H.; and Gogate, P.R. (2016). Intensified removal of copper from waste water using activated watermelon based biosorbent in the presence of ultrasound. *Ultrasonics Sonochemistry*, 30, 113-122.
51. Ani, J.U.; Okoro, U.C.; Aneke, L.E.; Onukwuli, O.D.; Obi, I.O.; Akpomie, K.G.; and Ofomatah, A.C. (2019). Application of response surface methodology for optimization of dissolved solids adsorption by activated coal. *Applied Water Science*, 9, 60.
52. Bakka, A.; Taleb, M.A.; Saffaj, N.; Laknifli, A.; Mamouni, R.; Benlhachemi, A.; Bakiz, B.; and Diane, Y. (2018). Patellidae shells waste as a biosorbent for the removal of aldrin pesticide from aqueous solutions. *Journal of Engineering Science and Technology* (*JESTEC*), 13(4), 925-942.
53. Vezentsev, A.I.; Thuy, D.M.; Peristaya, L.F.; Peristyj, V.A.; Alateya, A.T.; and Minh, P.T. (2019). Investigation of sorption of Cu^{2+}, Zn^{2+} and Cd^{2+} ions by a composite adsorbent obtained from bentonite-like clay and hydroxyapatite. *Journal of Engineering Science and Technology* (*JESTEC*), 14(1), 520-530.
54. Lagergren, S. (1989). About the theory of so-called adsorption of soluble substances. *Kungliga Svenska Vetenskapsakademies Handlingar*, 24(4), 1-39.
55. Ho, Y.S.; Wase, D.A.J.; and Forster, C.F. (1996). Kinetic studies of competitive heavy metal adsorption by sphagnum moss peat. *Environmental Technology*, 17, 71-77.
56. Muslim, A.; Aprilia, S.; Suha, T.A.; and Fitri, Z. (2017). Adsorption of Pb (II) ions from aqueous solution using activated carbon prepared from areca catechu

shell: Kinetic, isotherm and thermodynamic studies. *Journal of the Korean Chemical Society*, 61(3), 89-96.

57. Langmuir, I. (1918). The adsorption of gases on plane surface of glass, mica and platinum. *Journal of the American Chemical Society*, 40(9), 1361-1403.
58. Freundlich, H. (1906). Adsorption in solution. *The Journal of Physical Chemistry*, 57, 384-410.
59. Venegas-Sánchez, J.A.; Tagaya, M.; and Kobayashi, T. (2014). Ultrasound stimulus inducing change in hydrogen bonded crosslinking of aqueous polyvinyl alcohols. *Ultrasonics Sonochemistry*, 21(1), 295-309.
60. Wang, Z.; Pang, Y.; and Dlott, D.D. (2007). Hydrogen-Bond Disruption by Vibrational Excitations in Water, *The Journal of Physical Chemistry A*, 111 (17), 3196-3208.
61. Mohan, D.; Gupta, V.K.; Srivastava, S.K.; and Chander, S. (2001). Kinetics of mercury adsorption from wastewater using activated carbon derived from fertilizer waste. *Colloids and Surfaces A: Physicochemical and Engineering Aspects*, 177(2-3), 169-181.
62. Hubbe, M.A.; Azizian, S.; and Douven, S. (2019). Implications of apparent pseudo-second-order adsorption kinetics onto cellulosic materials: A review. BioResources, 14(3), 7582-7626.
63. Wang, H.; Zhou, A.; Peng, F.; Yu, H.; and Yang, J. (2007). Mechanism study on adsorption of acidified multi-walled carbon nanotubes to Pb(II). *The Journal of Colloid and Interface Science*, 316, 277-283.
64. Jasper, E.E., Ajibola, V.O.; and Onwuka, J.C. (2020). Nonlinear regression analysis of the sorption of crystal violet and methylene blue from aqueous solutions onto an agro-waste derived activated carbon. Applied Water Science, 10, 132.
65. Fierro, V.; Torné-Fernández, V.; Montané, D.; and Celzard, A. (2008). Adsorption of phenol onto activated carbons having different textural and surface properties. *Microporous and Mesoporous Materials*, 111(1-3), 276-284.
66. Liu, X.; Zhang, W.; and Zhang, Z. (2014). Preparation and characteristics of activated carbon from waste fiberboard and its use for adsorption of Cu(II). *Materials Letters*, 116, 304-306(2014).